water

MDPI

Article

The Performance of Satellite-Based Actual Evapotranspiration Products and the Assessment of Irrigation Efficiency in Egypt

Saher Ayyad [1,*], Islam S. Al Zayed [2], Van Tran Thi Ha [1,3] and Lars Ribbe [1]

1 Institute for Technology and Resources Management in the Tropics and Subtropics (ITT), Cologne University of Applied Sciences, 50679 Cologne, Germany; tranhavan@gmail.com (V.T.T.H.); lars.ribbe@th-koeln.de (L.R.)
2 National Water Research Center (NWRC), Cairo 13411, Egypt; eng_islam_sabry@yahoo.com
3 Department of Spatial Information Management and Modelling (RIM), Technical University of Dortmund, 44227 Dortmund, Germany
* Correspondence: saher.ayyad@hotmail.com; Tel.: +49-1794-325-744

Received: 7 August 2019; Accepted: 11 September 2019; Published: 14 September 2019

Abstract: Monitoring of crop water consumption, also known as actual evapotranspiration (ETa), is crucial for the prudent use of limited freshwater resources. Remote-sensing-based algorithms have become a popular approach for providing spatio-temporal information on ETa. Satellite-based ETa products are widely available. However, identifying an adequate product remains a challenge due to validation data scarcity. This study developed an assessment process to identify superior ETa products in agricultural areas in Egypt. The land cover product (MCD12Q1) from Moderate Resolution Imaging Spectroradiometer (MODIS) was evaluated and used to detect agricultural areas. The performances of three ETa products, namely: Earth Engine Evapotranspiration Flux (EEFlux), USGS-FEWS NET SSEBop ETa monthly product, and MODIS ETa monthly product (MOD16A2), were evaluated. The ETa values of these products were compared to previous ETa observations and evaluated using the integrated Normalized Difference Vegetation Index (iNDVI) on a seasonal and annual basis. Finally, the irrigation efficiency throughout Egypt was calculated based on the annual Relative Water Supply (RWS) index. Results reveal that the SSEBop monthly product has the best performance in Egypt, followed by the MOD16A2. The EEFlux overestimated ETa values by 36%. RWS had a range of 0.96–1.47, indicating high irrigation efficiency. The findings reported herein can assist in improving irrigation water management in Egypt and the Nile Basin.

Keywords: actual evapotranspiration; remote sensing; relative water supply; normalized difference vegetation index; land cover; Nile Delta and Nile Valley

1. Introduction

Approximately 70% of all global freshwater use is consumed by irrigated agriculture [1–4]. Water scarcity has become a limiting factor for agricultural production, especially in arid and semi-arid regions, where crop water consumption exceeds precipitation. These regions rely on water extracted from surface and/or groundwater sources to compensate for irrigation water deficits. The water crisis is even worse in regions of high political uncertainty, such as the Nile Basin, a region whose water management has become increasingly complex since the expansion of water infrastructure developments and the subsequent intensification of agricultural projects [5,6]. Egypt is the most downstream nation in the Nile Basin, and most of its freshwater inflow (≈97%) comes from outside its boundaries [7,8]. Omar and Moussa [9] claimed that the water shortage for different sectors in Egypt equaled to 13.5 Billion cubic meters (BCM) per year and expected this deficit to increase continuously.

The per capita water availability in Egypt is projected to be 500 cubic meters per year by 2025, which implies an absolute water-scarce situation [10,11]. Thus, Egypt's available water resources should be used in a manner that meets the demands of all water sectors.

Historically, irrigated agriculture has been considered an essential element of the economy and culture in Egypt [11]. Agricultural areas cover about 4% of the country's area [8,12,13] and consume over 85% of the national water share [2,14,15]. The agricultural sector contributes 17% to the country's Gross Domestic Product (GDP) and provides employment for about 40% of the labor force [16].

Water conveyance efficiency in the Egyptian irrigation system is about 70%, while field application efficiency has a range of 50%–60% [17,18]. These numbers are high since surface irrigation is the most commonly used technique in the country. Nevertheless, the water use system in some regions, such as the Nile Delta, is characterized by a high overall efficiency equivalent to 93% because of the water-reuse system [15]. Despite the high overall irrigation efficiency of the Egyptian irrigation system, the available data on water use in Egypt are considered rough estimates and not based on field measurements [19]. Irrigation management in Egypt is a challenge due to this data deficit. Given that Egypt's population is rapidly growing, El-Nashar and Hussien [20] have emphasized the need for proper estimation of the water demand for different crops to meet the increasing food demand. Within this context, the proper estimation of crop water consumption, also known as actual evapotranspiration (ETa), by using remote sensing data can support decision makers in developing methods to enhance water use efficiency.

Crop water demand is defined as the amount of applied water to an agricultural field to meet the needs of the crop's ETa [21,22]. ETa is a principal element of the hydrological cycle [23–25] and describes the actual evaporation process that occurs both on the surface of the bare soil or a water surface and from plants, i.e., plant leaf transpiration [21,24,26]. Both processes take place as a reaction to climate demand [23]. The proper estimation of the ETa in irrigation systems is a fundamental part of agricultural water management, water resources planning, water allocation, and water use efficiency studies, as it informs decision makers about the amount of crops' consumptive water use and enables them to better connect the available water resources to different land uses [23,27–30]. Several field-based methods were developed to measure ETa directly, such as lysimeter systems [31] and eddy covariance flux towers [32]. Evaporation pans [33] and Bowen ratio stations [34] are indirect methods for measuring ETa. However, these field methods are point measurements and restricted to the temporal and spatial scales from which they are observed [29,35–37]. Additionally, these methods need meteorological information gathered from ground stations, which present obstacles in poor regions [38].

Scholars agree that remote sensing data are of vital significance for providing spatio-temporal information on evapotranspiration [24,29,30,38–41]. Estimating ETa from remote sensing data started in the 1970s [42]. Over the years, scholars have developed and improved several remote sensing methods that are reproducible and beneficial for ETa estimates [43–51]. These improvements created less need for ground-based measurements and provided ETa estimates at high spatial resolutions that can help decision makers achieve better water resource management for large agricultural schemes [26,37]. Generally, using remote sensing data requires a validation based on ground-truth data. Given the lack of these ground-truth validation data, identifying an adequate method remains a challenge [29], particularly in the Nile Basin where data are scarce and unreliable [52].

Open-source ETa products are widely available and freely accessible. Some of these products include the Earth Engine Evapotranspiration Flux (EEFlux) [49], United States Geological Survey-Famine Early Warning Systems Network (USGS-FEWS NET) SSEBop Evapotranspiration products [51], the remotely sensed ETa monthly product MOD16A2 by the Numerical Terradynamic Simulation Group (NTSG) [53,54], the FAO Water Productivity through Open access of Remotely sensed derived data (WaPOR) [55], the Global Land Evaporation Amsterdam Model (GLEAM) [56–58], and the Satellite Application Facility on Land-Surface Analysis (LSA SAF) by the European Organization for the Exploitation of Meteorological Satellites [59]. Given that each ETa product has not been evaluated

using an Egyptian case, researchers and practitioners have yet to identify a better-performing product. The aforementioned products estimate the surface heat fluxes via satellite-derived Land-Surface Temperature (LST), and therefore represent one-source models. In two-source models, such as the Two-Source Energy Balance model (TSEB) [60], improvements have been made to benefit more from LST by individually estimating the sensible heat flux (H) and latent heat flux (LE) for the soil and canopy. However, these two-source models are not widely available yet, and therefore will not be used in this research.

Several studies to estimate the crop water requirements using different remote-sensing-based ETa estimation methods have been done in Egypt on local and regional scales [36,52,61–64]. In their 2011 study, Elhag et al. [36] applied the Surface Energy Balance System (SEBS) to estimate daily ETa and evaporation fractions over the agricultural areas in the Nile Delta in August 2007. The simulated daily ETa values provided by the SEBS model were compared with the ground-truth data (i.e., ninety-two data points recorded by lysimeter systems that are uniformly distributed throughout the Nile Delta) and the mean daily ETa value over the Delta region was estimated. Finally, the simulated daily ETa values provided by the SEBS model were compared with ground-truth data, and the mean daily ETa value over the Delta region was estimated. Another recent remote sensing study was conducted by Bastiaanssen et al. [63], who estimated ETa values from the operational Simplified Surface Energy Balance (SSEBop) for areas in the Nile Basin under water management from 2005 to 2010. They then calibrated the values of ETa estimates from SSEBop against the outputs from another model called ETLook [50] and adjusted them for interception energy. Recently, Droogers et al. [61] compiled different remote sensing ETa studies to assess national water information for Egypt. They have used the ETLook method with eight-day intervals to estimate the ETa for the entire year of 2007 over the irrigated areas in the Nile Valley and the Delta. However, no consensus on the variability of ETa estimates was found in the aforementioned studies.

The aim of this research, therefore, is to identify the best remote sensing ETa product that Egyptian stakeholders can use as a neutral tool to achieve the most efficient water management. The objectives of this paper are three-fold: (i) to identify the Egyptian agricultural areas; (ii) to evaluate the performance of three satellite-based ETa products (EEFlux, SSEBop, and MOD16A2) over these agricultural areas; and (iii) to assess irrigation efficiency in Egypt.

2. Materials and Methods

2.1. Study Area

Egypt is a hyper-arid country with temperatures ranging from 14 °C (in winter) to 30 °C (in summer) along its coastal regions. Conversely, inland areas vary in temperature between 7–43 °C and 0–18 °C in summer and winter, respectively [16]. Rainfall variability within the country is almost inconsequential since Egypt's Mediterranean coast is the only part of the country that receives rain—only 200 mm/year. Moving southwards, the Nile Delta receives very limited rainfall and only traces of rainfall from Cairo to the southern borders [16,65]. As shown in Figure 1, Egypt's major agricultural zone is in the Nile Delta and the Nile Valley [8,22,66]. The country has two cropping seasons, one in summer (the main cropping season, which has the highest water demand (April–September)), and the other in winter (October–March). Rice, cotton, maize, and sugar cane are the major crops of the summer season, while wheat, clover, and beans are planted in the winter season [8,66,67].

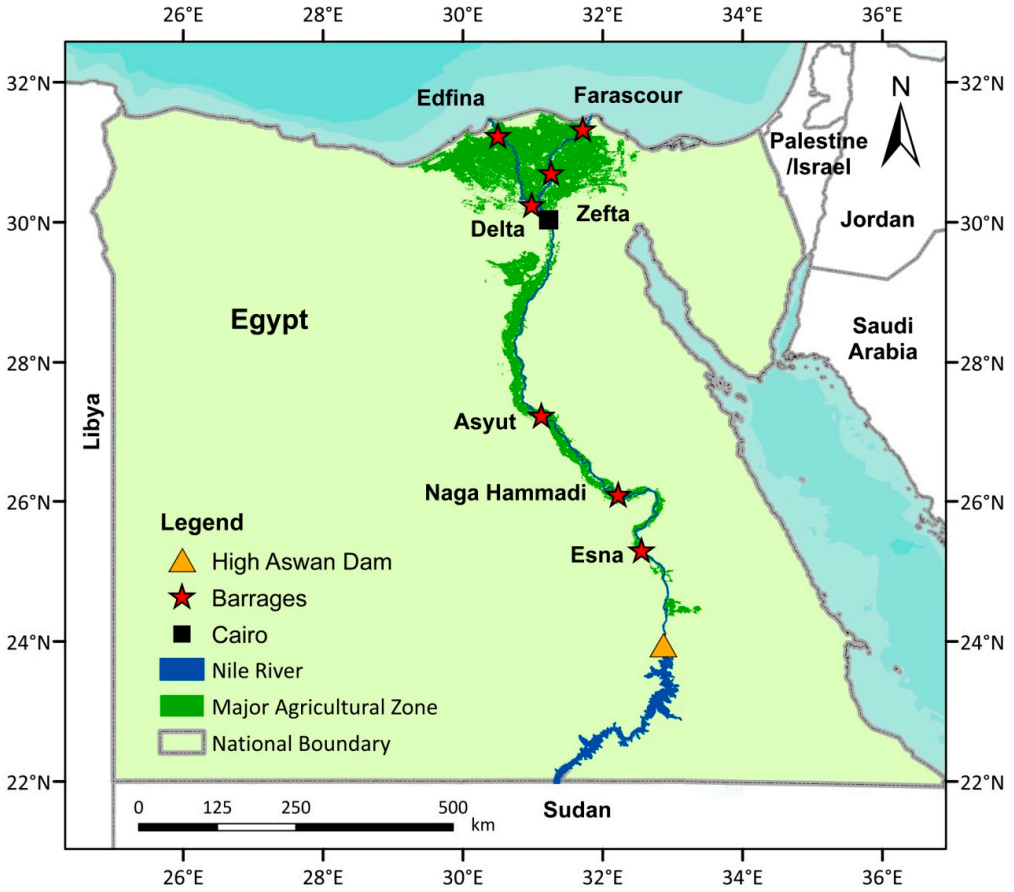

Figure 1. Location map of Egypt illustrating the major agricultural zone and irrigation infrastructure in the Nile Delta and the Nile Valley.

The irrigation infrastructure in Egypt starts upstream with Lake Nasser, which is controlled by the High Aswan Dam (HAD). Downstream of the HAD, several barrages control the water levels and water distribution systems. The canal system, downstream from the HAD, consists of major, branch, and distributary canals that divert water upstream of barrages to fields.

2.2. Selection and Description of Remote Sensing Products

Our study employs several remote sensing products of land cover, ETa, and the Normalized Difference Vegetation Index (NDVI) to identify the best performing ETa product. Table 1 shows the datasets which were selected for having longtime global coverage, different spatio-temporal resolutions, and public-domain sources.

Table 1. Description of the used remote sensing products.

Product	EEFlux	MOD16A2-Monthly	SSEBop-Monthly	Land Cover-MCD12Q1	NDVI-MOD13A3
Spatial resolution	30 m	1 km	(~1 km)	500 m	1 km
Temporal resolution	Daily	Monthly	Monthly	Annual	Monthly
Remote sensing observation	Landsat	MODIS	MODIS	MODIS	MODIS
Time period coverage	1983–present	2000–2014	2003–present	2000–2017	2000–present

2.2.1. Land Cover Dataset

Land cover datasets are necessary for delineating the extent of agricultural areas and their spatial-temporal distribution, as well as for estimating the ETa over these areas. We extracted the Terra and Aqua combined MODIS Land Cover dataset (MCD12Q1) Version 6 from the USGS portal in the HDF format [68,69]. The classification scheme Type1 Annual International Geosphere-Biosphere Programme (IGBP) was used. Al Zayed et al. [70] and Khalifa et al. [71] have also used the IGBP dataset and found it appropriate for large-scale areas in the Sudan and Ethiopia. The IGBP identifies 17 land cover classes, which include 11 natural vegetation classes, three developed and mosaicked land classes, and three non-vegetated land classes. Three MODIS grid system tiles (h20v05, h20v06, and h21v06) cover the whole country of Egypt. The three tiles were mosaicked into one raster map to analyze the land cover maps for the years from 2004 to 2017.

2.2.2. Actual Evapotranspiration Products

In this study, we analyzed, assessed, and applied three remote sensing ETa products to the Nile Delta and the Nile Valley in Egypt. The first product, the Earth Engine Evapotranspiration Flux (EEFlux) [72], features daily ETa estimates using Mapping Evapotranspiration at high Resolution with Internalized Calibration (METRIC) algorithm originally developed by Allen et al. [49]. EEFlux operates on the Google Earth Engine system for regional-scale estimates of the ETa using Landsat data. It has been developed by the consortium of the University of Nebraska-Lincoln, Desert Research Institute, and the University of Idaho in the United States of America [73]. The second remote sensing ETa product is SSEBop Evapotranspiration monthly product version 4, retrieved from the USGS-FEWS NET data portal [74]. This product stems from the operational Simplified Surface Energy Balance algorithm (SSEBop) that Senay et al. [51] developed. The third remote sensing ETa product is MOD16A2 by the Numerical Terradynamic Simulation Group (NTSG) [75], which was gathered monthly. The MOD16A2 product is derived from the Moderate Resolution Imaging Spectroradiometer (MODIS) satellite images using an improved evapotranspiration algorithm [53,54], which is based on the Penman–Monteith equation [76]. As illustrated, these products are derived from different ETa estimation methods. The EEFlux is derived from the surface energy balance model (METRIC), while the MOD16A2 and SSEBop products are based on the Penman–Monteith and the simplified surface energy balance methods, respectively.

2.2.3. Normalized Difference Vegetation Index (NDVI)

Our study takes advantage of the direct relationship between the ETa and the NDVI, which can also assess the performance of daily or seasonal ETa estimates from remote sensing data. We retrieved NDVI images of MODIS/Terra Vegetation Indices (MOD13A3) Monthly L3 Global 1 km in the sinusoidal projection (SIN) Grid V006 from the USGS portal [77] (see Table 1).

2.3. Methods of Evaluation for Remote Sensing Products

2.3.1. Land Cover

The obtained land cover images from the MCD12Q1 product were verified and compared with Google Earth historical images and another land cover product from GlobCover Land Cover Maps. However, the GlobCover is only available for 2005, 2006, and 2009 and was released by the European Space Agency Data User Element (ESA DUE) [78]. Furthermore, using the MCD12Q1, Egypt's total cropland area was calculated and compared with the official published data for cropland areas by the Central Agency for Public Mobilization and Statistics (CAPMAS) [79]. The CAPMAS is the official statistical agency of Egypt that collects, processes, analyzes, and disseminates statistical data at the national scale [80].

2.3.2. Actual Evapotranspiration

One of the limitations that this research faced was the absence of regional ground-truth data that can be used for validating the ETa products, for example, lysimeter systems or eddy covariance towers. Therefore, the present study developed a process to identify the best performing ETa product among the three selected products, as illustrated in Figure 2.

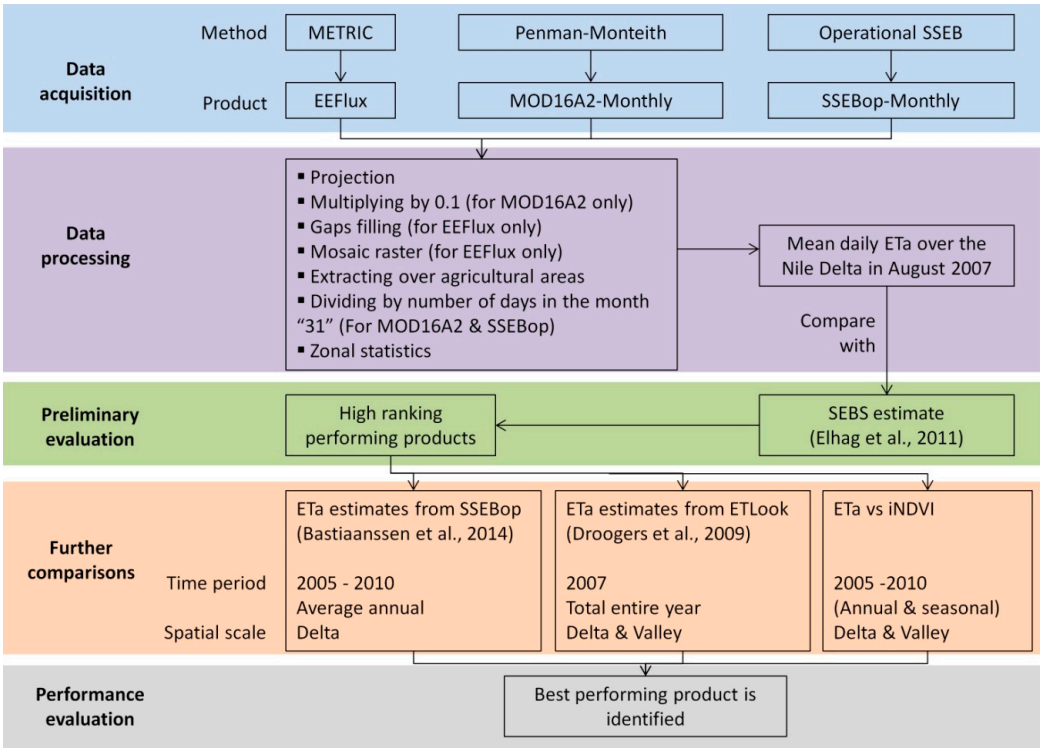

Figure 2. Evaluation process of three selected ETa product.

We initially compared the results from the three aforementioned ETa products with the estimated value derived from the SEBS model by Elhag et al. [36]. The average daily ETa values were estimated for the agricultural areas of the Nile Delta region for August 2007. We used the 2007 MCD12Q1 Landcover map to capture only the agricultural areas in the Delta. Using the ArcGIS 10.4 software (ESRI, Redlands, CA, USA) [81] throughout the whole process, we projected the three products and masked them over the agricultural areas in the Delta.

Using the raster calculator function of ArcGIS 10.4, we obtained the average daily value from the SSEBop monthly raster map and divided it by 31 because August has 31 days. Similarly, the MOD16A2 monthly raster map was multiplied by a factor of 0.1, as described by the user's guide [75], and then divided by 31. Five EEFlux tiles cover the Delta region: (path 176, row 39), (path 176, row 38), (path 177, row 38), (path 177, row 39), and (path 178, row 39). We used nine available ETa raster maps from the August 2007 EEFlux product as primary images (Table 2). Three images were derived from Landsat 5 images and another six from Landsat 7 images, in which there exists a Scan Line Corrector (SLC off-data) issue. The SLC off-data error occurred on 31 May 2003, producing data gaps within the produced Landsat 7 images [82]. To fix this issue, we decided to use the historical technique for filling gaps. For agricultural purposes, it is acceptable to choose a filling raster from more than one year prior to the date of the primary (SLC-off) raster, since many crops are rotated in multi-year cycles [83]. Hence, another four "filling" raster maps of August 2005, 2006, and 2007, were selected to close these gaps (Table 2). These filling raster maps were derived from Landsat 5 and have close values from the primary raster maps around the off-data lines. The gaps with zero values were extracted using the extract by attributes function (value = 0) and were then extracted by a mask over the filling raster maps.

Then we combined the resulting filled gaps to their primary raster maps using the mosaic function, ensuring that all gaps are closed. This produced at least one filled raster for each tile. It is important to highlight that both the primary and the filling images were chosen free of cloud cover (i.e., with 100% visibility), excluding two images that had a land cloud cover of 1% and 2%. Finally, we generated an average raster for the daily ETa values for each tile and clipped these to their respective tiles' borders. To obtain one raster, we mosaicked the five final raster maps into one, considering a mean value for the overlapped areas.

Table 2. EEFlux images used.

Tile	Primary Raster Maps	Cloud (%)	Date	Filling Raster Maps	Cloud (%)	Date
1	LE71760392007223ASN00	0	11.08.2007	LT51760392005225MTI00	0	13.08.2005
1	LE71760392007239ASN00	0	27.08.2007			
2	LE71760382007239ASN00	0	27.08.2007	LT51760382007215MTI00	2	03.08.2007
2	LE71760382007223ASN00	0	11.08.2007			
3	LT51770382007238MTI00	0	26.08.2007			
4	LE71770392007214ASN00	0	02.08.2007	LT51770392007222MTI00	0	10.08.2007
4	LT51770392007222MTI00	0	10.08.2007			
5	LT51780392007213MTI00	1	01.08.2007			
5	LE71780392007237ASN00	0	25.08.2007	LT51780392006226MTI00	0	14.08.2006

Based on the resultant mean daily ETa values from the aforementioned three ETa products, we ranked the products according to how much their deviation percentage varied from the SEBS model estimate [36]. The highly ranked performing products (<10% deviation) were then selected for further evaluation.

To ensure the validity of our ETa products for the Egyptian case, we subsequently compared the highly ranked performing products with the existing ETa estimations from Bastiaanssen et al. and Droogers et al. [61,63]. The former calculated an average annual ETa value for the Nile Delta between 2005 and 2010. The latter estimated the best ETa value for both the Nile Delta and the Valley regions for the whole year of 2007. Variations in the methods of the aforementioned ETa studies impair rigorous collation based entirely on their results. Therefore, we incorporated NDVI values as further indicators for the products' performances.

Al Zayed et al. [29] suggest a robust method for assessing the performance of ETa estimates over agricultural areas using the integrated NDVI (iNDVI): The higher the ETa, the greater the iNDVI. This approach was used in several pieces of literature showing a high correlation between total seasonal ETa and iNDVI [29,84,85]. According to Senay et al. [26], the NDVI or Vegetation index model is suitable for estimating ETa in arid and semi-arid regions because ET is dominated by transpiration. In this paper, integrated NDVI is considered to be an extra comparison indicator for evaluating the performance of different remote sensing-based ETa products, since the correlation of integrated NDVI and seasonal ETa is significant to understand the water requirement of different crop seasons for better water allocation and management. In addition to seasonal comparisons of ETa and iNDVI values, the present study proposes a comparison on an annual basis. We performed both seasonal (summer) and annual comparisons for the period between 2005 and 2010 over agricultural areas in the Nile Delta and Valley. Three data sets were considered: 72 NDVI images, 144 ETa raster maps, and six annual land cover images. The mean seasonal and annual ETa values were plotted versus their respective iNDVI, and later we performed a linear regression to examine the correlation between the ETa and iNDVI values. The ETa product with the best correlation with iNDVI was identified as the best performing ETa product and further used to assess irrigation water use throughout Egypt.

2.4. Assessing the Irrigation Efficiency

CAPMAS provides data on the allocated annual irrigation water quantities at Aswan, along canals and onto the fields, for the period between 2004 and 2017 [14]. In Egypt, field irrigation quantities are calculated by multiplying the water rations with the cultivated areas for each crop, including losses

resulting from leakage, excess surface water, and leaching water. Subsequently, canal quantities are calculated by adding 10%–20% to the field irrigation quantities, to compensate for the evaporation and leakage losses [86]. At Aswan, CAPMAS defines irrigation water quantities as the amount of released water from the High Aswan Dam to irrigate agricultural areas of the whole country [86].

Using the best performing product, we calculated the annual ETa estimates for the same period for all agricultural areas in Egypt. Agricultural areas were captured using the land cover MCD12Q1 product. Then, we compared the annual ETa estimates to allocated annual irrigation water quantities. To further assess the performance of the irrigation water efficiency on an annual basis for the period from 2004 to 2017, we referenced the irrigation efficiency indicator (i.e., the Relative Water Supply (RWS)) [87,88]. Several studies also apply the RWS to address irrigation efficiency [70,89–91]. RWS is represented as:

$$\text{RWS} = \frac{\text{total water supply (irrigation supply + precipitation)}}{\text{total water demand (crop evapotranspiration(ETc))}}. \quad (1)$$

Since practically all agricultural activities in Egypt depend on irrigation water [16], it is reasonable to equate the CAPMAS's published irrigation water qualities with the total water supply. According to Moreno-Pérez and Roldán-Cañas [91] and Al Zayed et al. [70], RWS values with the ranges of 0.9 to 1.2, 1.2 to 1.4 and >1.4 indicate adequate, fairly good and surplus irrigation efficiencies, respectively, by using ETa instead of ETc.

3. Results and Discussion

3.1. Assessment of Agricultural Lands Obtained from Land Cover Data

After verifying and comparing the MCD12Q1 images with historical Google Earth images and GlobCover Land Cover Maps, three vegetation classifications were selected to represent the agricultural areas: croplands, cropland–natural vegetation mosaics, and grasslands (ID No: 12, 14, and 10, respectively). Subsequently, we compared the total annual agricultural area derived from the land cover product MCD12Q1 to the official cropland data published by the CAPMAS for Egypt in the period between 2004 and 2017. The result showed that the official CAPMAS dataset has a greater crop coverage extent than our calculated one. The former has between 2.7% and 7.5% more crop coverage than the latter. However, there is a significant correlation between our calculations and the official data sets (see Figure 3). Hence, our study used the MCD12Q1 for extracting agricultural areas for the subsequent steps to evaluate ETa products.

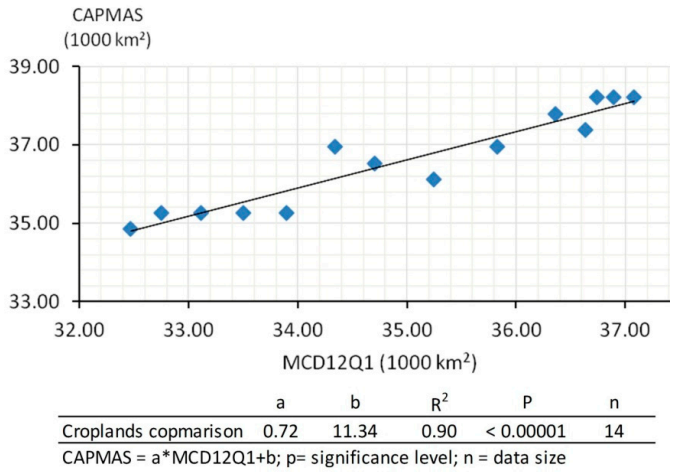

	a	b	R^2	P	n
Croplands copmarison	0.72	11.34	0.90	< 0.00001	14

CAPMAS = a*MCD12Q1+b; p= significance level; n = data size

Figure 3. Correlation between the agricultural areas estimated by the MCD12Q1 land cover and official Egyptian statistics by the CAPMAS (2004–2017).

3.2. Evaluation of ETa Products

3.2.1. Assessment Based on Previous Observations

Average Daily ETa Values in August 2007

The resulting spatial distribution of the ETa over the Nile Delta region from all products showed high ETa values throughout the middle of the Delta's "old land cultivation" and low values in the peripheral areas of the "new reclaimed agricultural land" (Figure 4). This spatial distribution agrees well with the several remote sensing ETa studies [52,61,63,64,92,93]. However, the SEBS model resulted in higher daily ET values than expected in areas of the peripheral Nile Delta. Elhag et al. [36] identified this as one of the limitations of the SEBS model and stated that in newly reclaimed lands at the fringe of the delta, this model tends to estimate the potential ET rather than the actual ET. ETa estimations of the SEBS model were highly correlated with ground measurements over the entire Nile Delta region, as reflected in the regression equation ($Y = 0.9871x$ and $R^2 = 0.8412$). High correlation could, in this case, be explained by the lack of ground-truth points in the peripheral areas, where water is less available and agriculture less intensive [94]. Hence, the present study uses an adjusted SEBS model estimated mean daily ETa value of 4.40 mm/day compared to the model's initial value (4.35 mm/day). Table 3 shows the results of the average daily ETa estimation using the three products and their corresponding deviation percentage from the SEBS model adjusted value.

Table 3. Mean daily ETa values estimated with the three products compared to the adjusted value by the SEBS model in August 2007.

Dataset	Mean ETa (mm/day)	Deviation (%)
SEBS model (adjusted)	4.40	-
MOD16A2—monthly	5.04	3.86
EEFlux	6.00	36.36
SSEBop—monthly	4.37	0.68

According to the calculated deviation percentages, the SSEBop monthly product is the best performing product with the lowest deviation percentage (0.68%). The MOD16A2 monthly product overestimates the ETa. However, it is the second-best performing product, with a deviation of 3.86%. The EEFlux ETa estimate deviates significantly from the SEBS adjusted model by 36.36%. Figure 4 shows the mean daily ETa estimated values of the three selected products over the Nile Delta in August 2007. In a close-by region with a similar climate pattern, Al Zayed et al. [29] carried out a comparative study between four different ETa estimation methods over the Gazira irrigation scheme in Sudan. That study also found the SSEB method to be the best performing method for estimating ETa and observed that the METRIC method overestimated the ETa. Given the high deviation percent of the EEFlux, as well as the long processing times, we excluded the product from further evaluation steps. At this stage, the SSEBop and MOD16A2 monthly products were selected for further comparisons in the present study.

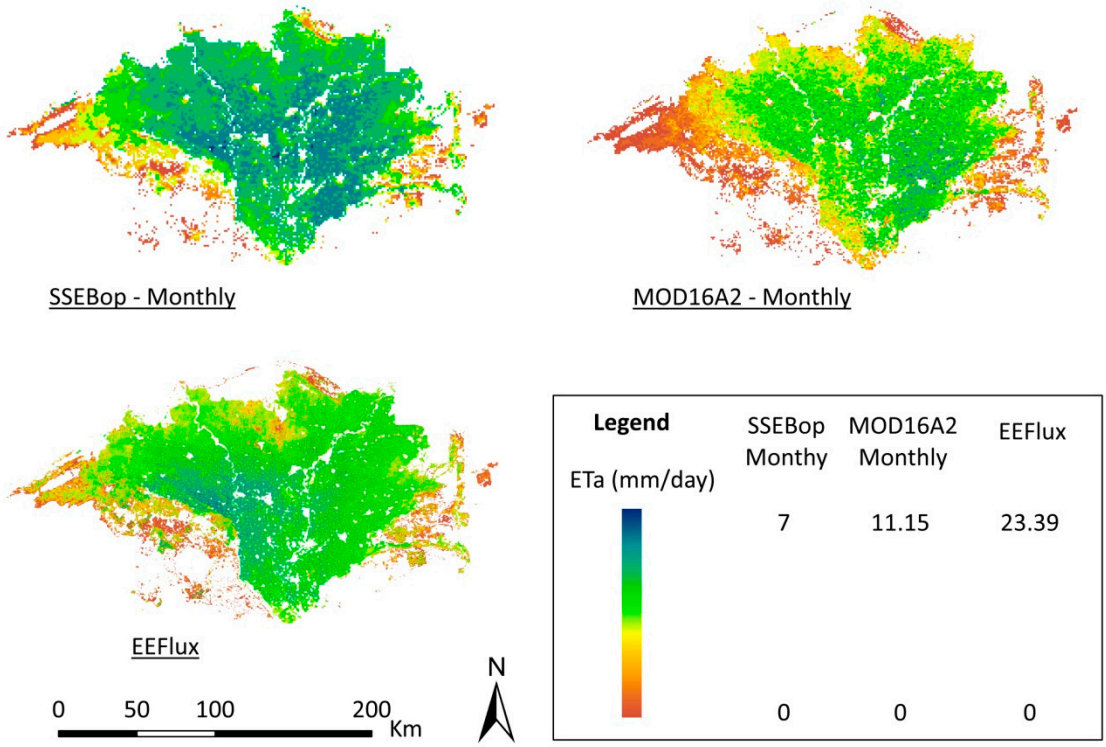

Figure 4. Mean daily Eta, estimated by the three selected products over the Nile Delta in August 2007.

Average Annual ETa Estimation during the 2005–2010 Period

We used both the SSEBop and MOD16A2 monthly products to estimate the average annual ETa throughout the entire Nile Delta from 2005 to 2010. The average agricultural area (extracted from the land cover MCD12Q1 product) for the same time period reached 21,255.13 km^2. The estimated average annual ETa of the SSEBop and MOD16A2 monthly products is 19.82 and 18.27 km^3, respectively. These values compare well with the estimate of 19 km^3 by Bastiaanssen et al. [63]. In other words, the two products show reasonable performance at this stage of comparison.

Average Annual ETa Estimation in 2007

We estimated the average ETa in 2007 for the Nile Valley and Delta regions. The croplands area extracted from the land cover MCD12Q1 product totaled 32,688.59 km^2. Droogers et al. [61] assumed that the irrigated areas are all pixels with a range of 200 < ET < 1500 mm. This led to an estimated area of 31,042.00 km^2. They then compared the ETLook results with the other remote sensing ETa estimates and determined that the best ETa estimate for 2007 is 30.2 km^3. This estimate is very close to the SSEBop and MOD16A2 estimates of 30.81 and 28.92 km^3, respectively. However, the SSEBop estimate is slightly better, as it comes closer to the best ETa estimate by Droogers et al. [61].

3.2.2. Assessment Based on iNDVI

We compared the SSEBop and MOD16A2 monthly products to the iNDVI on a seasonal and annual basis for the period between 2005 and 2010. Results showed that the SSEBop has higher correlations with seasonal and annual iNDVI than the MOD16A2 (Figure 5). The spatial distribution for both ETa products and the iNDVI, averaged for the period from 2005 to 2010, are shown in Figure 6.

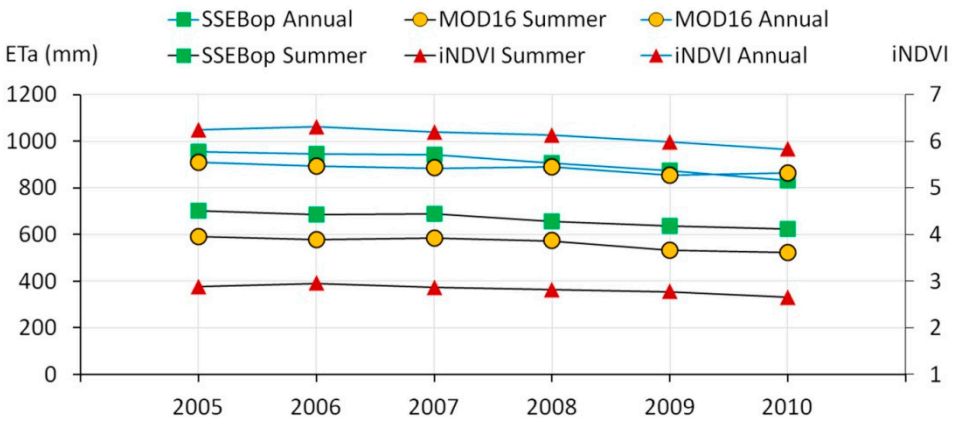

ETa product/season	a	b	R^2	P	n
SSEBop Annual	263.02	-698.97	0.94	< 0.005	6
MOD16 Annual	92.30	317.14	0.70	< 0.05	6
SSEBop Summer	269.25	-95.35	0.81	< 0.05	6
MOD16 Summer	244.57	-128.30	0.74	< 0.05	6

ETa = a*iNDVI+b; p= significance level; n = data size

Figure 5. Correlation between the ETa and the iNDVI on a seasonal and annual basis from 2005 to 2010.

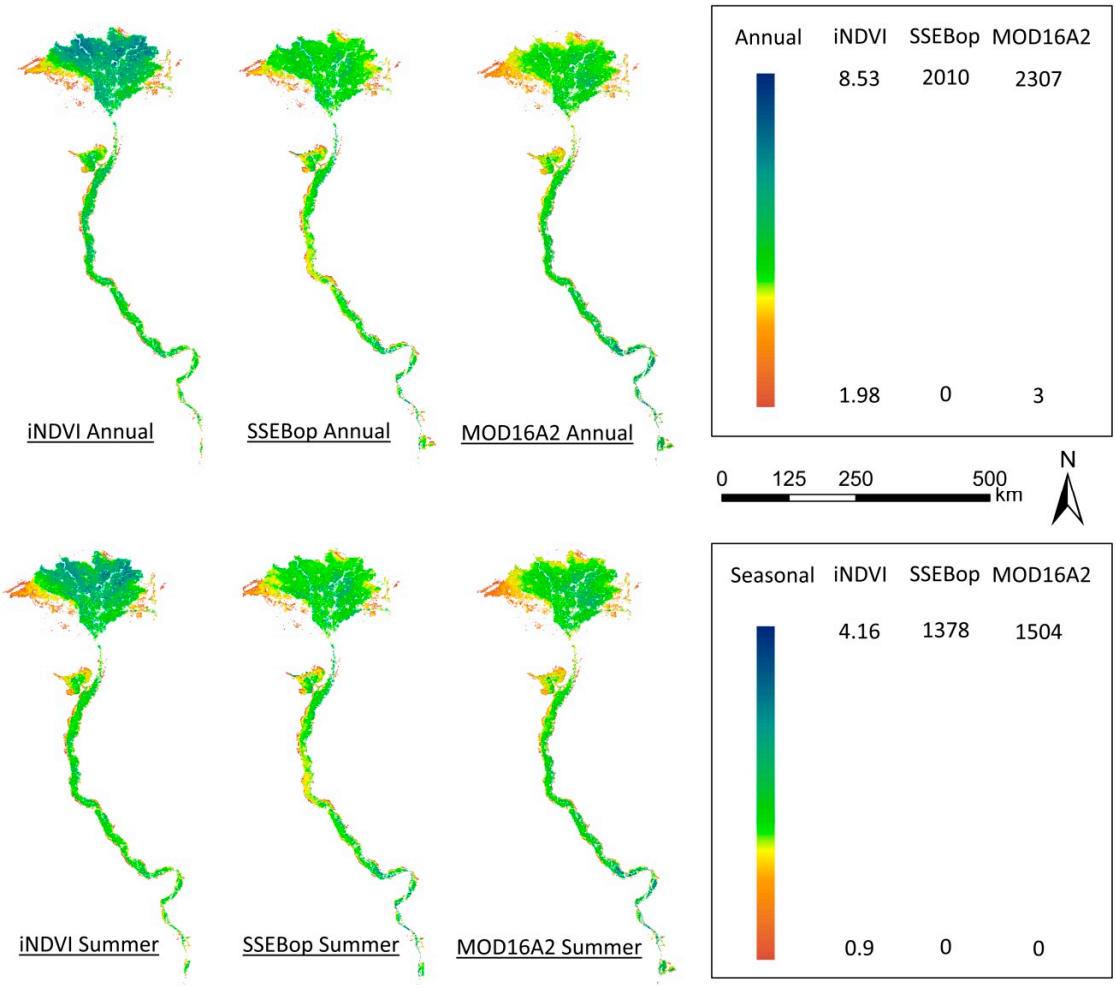

Figure 6. The average annual and seasonal ETa from the SSEBop and MOD16A2 products against the iNDVI over agricultural areas in the Nile Delta and Valley from 2005 to 2010.

Results of the ETa product's evaluation revealed that EEFlux overestimates the ETa values. The SSEBop and MOD16A2 provide reasonable estimations for the ETa. However, the MOD16A2's monthly product is not as favorable since it provides both overestimated and/or underestimated ETa values. The SSEBop performed slightly better in all applied comparisons. Therefore, we recommend it as a reliable product with high performance to estimate the actual evapotranspiration in such a data-scarce region, where agriculture is one of the most important activities and a primary water user. Researchers are advised to expand their toolsets to include remote sensing precipitation products and to investigate more ETa products. Performance of the same ETa products should be tested over other agricultural regions in the Nile Basin, to have a better understanding of the basin's entire water balance. Investing in ground-truth field measures (e.g., lysimeter systems or eddy covariance towers) is highly recommended to perform a rigid validation of the remote sensing ETa products. Furthermore, our study considers the NDVI as a sound indicator to assess the performance of ETa products. However, evaluating ET estimates should not be based solely on NDVI. Finally, the study was performed based on the assumption that an entire pixel is irrigated, while future research can enhance its data resolution by considering sub-pixel fractions.

3.3. Calculating the Irrigation Efficiency of Egypt

For a better understanding of agricultural water demand, the SSEBop monthly product was used to estimate the annual ETa throughout all agricultural areas in Egypt. For the period between 2004 and 2017, we plotted the annual ETa estimates against the allocated annual irrigation water quantities at Aswan, along canals, and onto the fields. Results showed that in most years, the supplied volume of the irrigation water is greater than the estimated actual evapotranspiration (between 17% and 47% higher), except for 2005 and 2011 (see Figure 7).

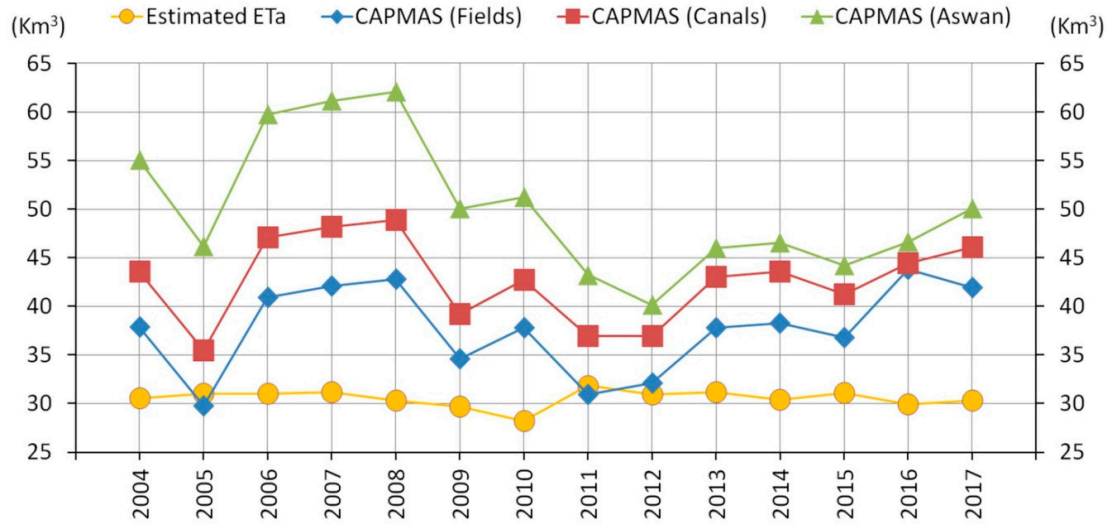

Figure 7. The annual ETa from SSEBop and the irrigation data published by CAPMAS for different scales.

To explain why ETa estimates differ from the actual volumes of the allocated irrigation water, the following points were assumed:

1. Fluctuating in- and outflow volumes at the HAD correspond generally with low irrigation water allocation during some years. This difference could be explained by the Egyptian drought management policy for HAD, which reduces water releases by 5%, 10%, and 15% if the storage volume upstream the dam falls below 60, 55, and 50 billion cubic meters, respectively [16,95].
2. The low field application efficiency (50%–60%) of surface irrigation methods, particularly in Egypt [17,18]. Agricultural old lands in the Nile Delta and Valley, which dominate the main

cultivated areas, lack adequate irrigation practices and modern irrigation techniques, leading to a reduction in their irrigation efficiency on the field scale [96,97].

3. The field irrigation quantities provided by CAPMAS account for losses associated with leakage, excess surface water, and leaching water, but these losses are excluded from our ETa estimates.

Our ETa values were estimated based on the delineated cropland area from the MCD12Q1 product, which was found to be smaller than the official cropland area provided by CAPMAS, as mentioned in Section 3.1.

The RWS values range from 0.96 to 1.47, with an average value of 1.23 from 2004 to 2017, which is considered as fairly good irrigation efficiency. Figure 8 shows the temporal variation of the RWS values. As can be seen, for the years 2005, 2009, 2011, 2012, and 2015, the values of the RWS imply adequate irrigation efficiency (from 0.9 to 1.2). In 2004, 2006, 2007, 2010, 2013, 2014, and 2017, the RWS results demonstrate fairly good irrigation efficiency (1.2 > RWS > 1.4). An over-irrigation situation (RWS > 1.4) occurred in 2008 and 2016.

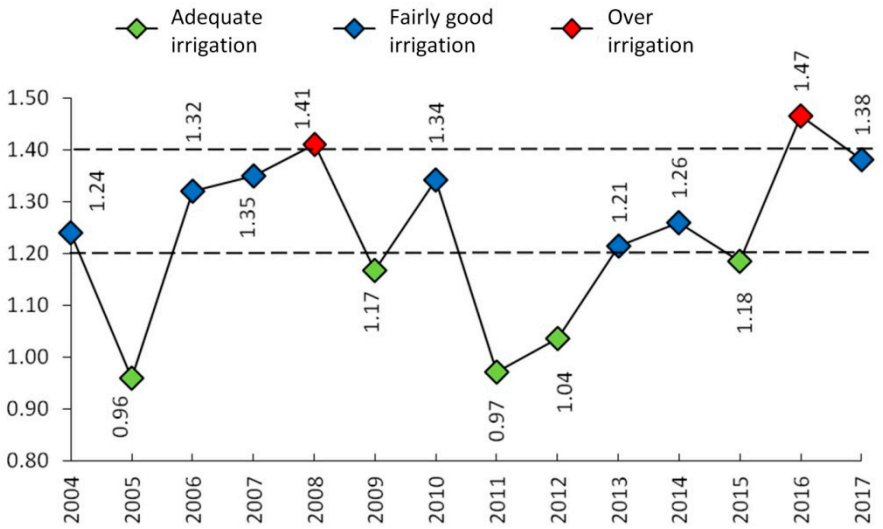

Figure 8. The temporal variation for the annual Relative Water Supply (RWS) for irrigated areas in Egypt (2004–2017).

Although surface irrigation is the most common irrigation technique [97], the overall Egyptian irrigation efficiency calculated from 2004 to 2017 is about 81% (RWS ≅ 1.23), indicating high irrigation efficiency. This value does not account for the high degree of reuse of drainage flow. As stated by Molle et al. [15], the overall irrigation efficiency could reach up to 93% in some regions, such as the Nile Delta, when considering the drainage water-reuse. Generally, the recycling agricultural return flow is determined as the effective water-saving technology to enhance the irrigation efficiency [98,99]. In Egypt, the agricultural drainage water goes back into the system by pumping it to the main canals. However, around 25% (officially and unofficially) has relatively good water quality and is used once again for irrigation, which is considered to be an integral addition to water sources, while the remaining water is delivered to the Mediterranean Sea and/or the Northern lakes [15,97]. Furthermore, the continuous expansion of the usage of the covered drains contributes to the high overall efficiency by reducing water losses resulting from evaporation, leakage of waterways, and excess irrigation water [80,86].

4. Conclusions

We analyzed three remote sensing ETa products and evaluated them according to the Egyptian agricultural areas of the Nile Delta and the Nile Valley. The products included the Earth Engine Evapotranspiration Flux (EEFlux), the USGS-FEWS NET SSEBop actual evapotranspiration monthly

product, and the remotely sensed ETa monthly product MOD16A2. Agricultural areas were delineated with the help of the land cover product (MCD12Q1). We compared the total agricultural areas estimated by MCD12Q1 to the official CAPMAS statistics from 2004 to 2017. This comparison indicated a significant correlation between the two data sets. The study used literature-based ETa values from previous studies to compare the ETa products. To further evaluate the performance of the tested products, we chose the NDVI product (MOD13A3) as an additional indicator. Results showed that EEFlux ETa estimations produce overestimations for the ETa values. Conversely, the SSEBop and MOD16A2 products provided close estimates for the ETa throughout the Nile Delta and Valley. The SSEBop monthly product performed slightly better in the applied comparisons, and, therefore, it was identified as the best performing product among those evaluated.

We used the SSEBop monthly product to assess irrigation efficiency in Egypt. The annual ETa values were estimated over the agricultural areas throughout Egypt from 2004 to 2017. Then, we compared the ETa estimates to the CAPMAS official statistics on the allocated irrigation water at Aswan, in canal heads, and at the field level. Results showed that the supplied irrigation water quantities, in most years, are much higher than the estimated ETa. In addition, the irrigation efficiency indicator (RWS) was calculated to be able to assess the performance of the irrigation water efficiency on an annual basis for the same period. The RWS results indicated a high irrigation efficiency in Egypt.

Author Contributions: Conceptualization, S.A., L.R., and I.S.A.Z.; methodology, S.A., I.S.A.Z., and V.T.T.V.; software, S.A.; formal analysis, S.A.; investigation, S.A.; data curation, S.A.; writing—original draft preparation, S.A.; writing—review and editing, I.S.A.Z., V.T.T.V., and L.R., and S.A.; visualization, S.A.; supervision, L.R. and V.T.T.V.; project administration, S.A. and L.R.; funding acquisition, L.R. and S.A.

Funding: The first author is very thankful for the German Academic Exchange Service (DAAD) for sponsoring the travel expenses related to the research. The APC was funded by the Institute for Technology and Resources Management in the Tropics and Subtropics (ITT), Cologne, Germany.

Acknowledgments: The authors would like to express their gratitude towards all open access satellite-based data providers for offering the datasets used in this study.

Conflicts of Interest: The authors declare no conflict of interest.

References

1. Frenken, K.; Gillet, V. *Irrigation Water Requirement and Water Withdrawal by Country*; AQUASTAT Report; Food and Agriculture Organization of the United Nation: Rome, Italy, 2012.
2. World Bank. World Development Indicators. Available online: http://wdi.worldbank.org/table/3.5 (accessed on 27 July 2018).
3. Bruinsma, J. *World Agriculture: Towards 2015/2030: An FAO Study*; Earthscan Publications Ltd.: London, UK, 2017.
4. WWAP (United Nations World Water Assessment Programme)/UN-Water. *The United Nations World Water Development Report 2018: Nature-Based Solutions for Water*; UNESCO: Paris, France, 2018.
5. Hamouda, M.A.; Nour El-Din, M.M.; Moursy, F.I. Vulnerability Assessment of Water Resources Systems in the Eastern Nile Basin. *Water Resour. Manag.* **2009**, *23*, 2697–2725. [CrossRef]
6. Basheer, M.; Wheeler, K.G.; Ribbe, L.; Majdalawi, M.; Abdo, G.; Zagona, E.A. Quantifying and evaluating the impacts of cooperation in transboundary river basins on the Water-Energy-Food nexus: The Blue Nile Basin. *Sci. Total Environ.* **2018**, *630*, 1309–1323. [CrossRef] [PubMed]
7. Amer, S.E.-D.; Arsano, Y.; El-Battahani, A.; Hamad, O.E.-T.; Hefny, M.A.E.-M.; Tamrat, I.; Mason, S.A. Sustainable development and international cooperation in the Eastern Nile Basin. *Aquat. Sci.* **2005**, *67*, 3–14. [CrossRef]
8. FAO AQUASTAT. FAO's Information System on Water and Agriculture. Available online: http://www.fao.org/nr/water/aquastat/countries_regions/EGY/ (accessed on 11 July 2018).
9. Omar, M.E.D.M.; Moussa, A.M.A. Water management in Egypt for facing the future challenges. *J. Adv. Res.* **2016**, *7*, 403–412. [CrossRef] [PubMed]
10. Falkenmark, M.; Widstrand, C. Population and water resources: A delicate balance. *Popul. Bull.* **1992**, *47*, 1–36. [PubMed]

11. Hefny, M.; Amer, S.E.-D. Egypt and the Nile Basin. *Aquat. Sci.* **2005**, *67*, 42–50. [CrossRef]
12. El-Kawy, O.A.; Rød, J.K.; Ismail, H.A.; Suliman, A.S. Land use and land cover change detection in the western Nile delta of Egypt using remote sensing data. *Appl. Geogr.* **2011**, *31*, 483–494. [CrossRef]
13. World Bank. World Development Indicators. Available online: http://wdi.worldbank.org/table/3.2 (accessed on 27 July 2018).
14. Central Agency for Public Mobilization and Statistics (CAPMAS). Irrigation Data. Available online: http://www.capmas.gov.eg/Pages/IndicatorsPage.aspx?Ind_id=2401 (accessed on 25 September 2018).
15. Molle, F.; Gaafar, I.; El-Agha, D.E.; Rap, E. The Nile delta's water and salt balances and implications for management. *Agric. Water Manag.* **2018**, *197*, 110–121. [CrossRef]
16. MWRI. *Water for the Future. National Water Resources Plan 2017*; Ministry of Water Resources and Irrigation: Cairo, Egypt, 2005.
17. Brouwer, C.; Prins, K.; Heibloem, M. *Irrigation Water Management: Irrigation Scheduling*; FAO: Rome, Italy, 1989; pp. 14–92.
18. SADS. *Sustainable Agricultural Development Strategy towards 2030 (SADS)*; Agricultural Research & Development Council, Arab Republic of Egypt, Ministry of Agriculture & Land Reclamation: Cairo, Egypt, 2009.
19. Allam, M.N.; Allam, G.I. Water Resources in Egypt: Future Challeges and Opportunities. *Water Int.* **2007**, *32*, 205–218. [CrossRef]
20. El-Nashar, W.Y.; Hussien, E.A. Estimating the potential evapo-transpiration and crop coefficient from climatic data in Middle Delta of Egypt. *Alex. Eng. J.* **2013**, *52*, 35–42. [CrossRef]
21. Allen, R.G.; Pereira, L.S.; Raes, D.; Smith, M. *Crop Evapotranspiration-Guidelines for Computing Crop Water Requirements-FAO Irrigation and Drainage Paper 56*; FAO: Rome, Italy, 1998; Volume 300, p. D05109.
22. Gad, H.E.; El-Gayar, S.M. Climate parameters used to evaluate the evapotranspiration in delta central zone of Egypt. In Proceedings of the Fourteenth International Water Technology Conference, IWTC14, Cairo, Egypt, 21–23 March 2010; pp. 529–548.
23. Hanson, R.L. Evapotranspiration and droughts. *US Geol. Surv. Water Supply Pap.* **1991**, *2375*, 99–104.
24. Immerzeel, W.W.; Droogers, P.; Gieske, A.S.M. *Remote Sensing and Evapotranspiration Mapping: State of the Art*; FutureWater: Wageningen, The Netherlands, 2006.
25. Maeda, E.E.; Wiberg, D.A.; Pellikka, P.K.E. Estimating reference evapotranspiration using remote sensing and empirical models in a region with limited ground data availability in Kenya. *Appl. Geogr.* **2011**, *31*, 251–258. [CrossRef]
26. Senay, G.B.; Leake, S.; Nagler, P.L.; Artan, G.; Dickinson, J.; Cordova, J.T.; Glenn, E.P. Estimating basin scale evapotranspiration (ET) by water balance and remote sensing methods. *Hydrol. Process.* **2011**, *25*, 4037–4049. [CrossRef]
27. Bashir, M.A.; Hata, T.; Tanakamaru, H.; Abdelhadi, A.W.; Tada, A. Satellite-based energy balance model to estimate seasonal evapotranspiration for irrigated sorghum: A case study from the Gezira scheme, Sudan. *Hydrol. Earth Syst. Sci.* **2008**, *12*, 1129–1139. [CrossRef]
28. Salama, M.A.; Yousef, K.M.; Mostafa, A.Z. Simple equation for estimating actual evapotranspiration using heat units for wheat in arid regions. *J. Radiat. Res. Appl. Sci.* **2015**, *8*, 418–427. [CrossRef]
29. Al Zayed, I.S.; Elagib, N.A.; Ribbe, L.; Heinrich, J. Satellite-based evapotranspiration over Gezira Irrigation Scheme, Sudan: A comparative study. *Agric. Water Manag.* **2016**, *177*, 66–76. [CrossRef]
30. Bastiaanssen, W.G.M.; Noordman, E.J.M.; Pelgrum, H.; Davids, G.; Thoreson, B.P.; Allen, R.G. SEBAL Model with Remotely Sensed Data to Improve Water-Resources Management under Actual Field Conditions. *J. Irrig. Drain. Eng.* **2005**, *131*, 85–93. [CrossRef]
31. Pruitt, W.O.; Angus, D.E. Large Weighing Lysimeter for Measuring Evapotranspiration. *Trans. ASAE* **1960**, *3*, 13–15.
32. Swinbank, W.C. The measurement of vertical transfer of heat and water vapor by eddies in the lower atmosphere. *J. Meteorol.* **1951**, *8*, 135–145. [CrossRef]
33. Snyder, R.L. Equation for Evaporation Pan to Evapotranspiration Conversions. *J. Irrig. Drain. Eng.* **1992**, *118*, 977–980. [CrossRef]
34. Fritschen, L.J. Accuracy of Evapotranspiration Determinations by the Bowen Ratio Method. *Int. Assoc. Sci. Hydrol. Bull.* **1965**, *10*, 38–48. [CrossRef]

35. Folhes, M.T.; Rennó, C.D.; Soares, J.V. Remote sensing for irrigation water management in the semi-arid Northeast of Brazil. *Agric. Water Manag.* **2009**, *96*, 1398–1408. [CrossRef]
36. Elhag, M.; Psilovikos, A.; Manakos, I.; Perakis, K. Application of the Sebs Water Balance Model in Estimating Daily Evapotranspiration and Evaporative Fraction from Remote Sensing Data Over the Nile Delta. *Water Resour Manag.* **2011**, *25*, 2731–2742. [CrossRef]
37. McShane, R.R.; Driscoll, K.P.; Sando, R. *A Review of Surface Energy Balance Models for Estimating Actual Evapotranspiration with Remote Sensing at High Spatiotemporal Resolution over Large Extents*; Scientific Investigations Report 2017-5087; U.S. Geological Survey: Reston, VA, USA, 2017; 19p.
38. El-Shirbeny, M.A.; Alsersy, M.A.; Saleh, N.H.; Abu-Taleb, K.A. Changes in irrigation water consumption in the Nile Delta of Egypt assessed by remote sensing. *Arab. J. Geosci.* **2015**, *8*, 10509–10519. [CrossRef]
39. Allen, R.G.; Irmak, A.; Trezza, R.; Hendrickx, J.M.H.; Bastiaanssen, W.; Kjaersgaard, J. Satellite-based ET estimation in agriculture using SEBAL and METRIC. *Hydrol. Process.* **2011**, *25*, 4011–4027. [CrossRef]
40. Bezerra, B.G.; da Silva, B.B.; dos Santos, C.A.C.; Bezerra, J.R.C. Actual Evapotranspiration Estimation Using Remote Sensing: Comparison of SEBAL and SSEB Approaches. *Adv. Remote Sens.* **2015**, *4*, 234–247. [CrossRef]
41. Lian, J.; Huang, M. Comparison of three remote sensing based models to estimate evapotranspiration in an oasis-desert region. *Agric. Water Manag.* **2016**, *165*, 153–162. [CrossRef]
42. Li, Z.-L.; Tang, R.; Wan, Z.; Bi, Y.; Zhou, C.; Tang, B.; Yan, G.; Zhang, X. A Review of Current Methodologies for Regional Evapotranspiration Estimation from Remotely Sensed Data. *Sensors* **2009**, *9*, 3801–3853. [CrossRef]
43. Kalma, J.D.; Jupp, D.L.B. Estimating evaporation from pasture using infrared thermometry: Evaluation of a one-layer resistance model. *Agric. For. Meteorol.* **1990**, *51*, 223–246. [CrossRef]
44. Menenti, M.; Choudhury, B. Parameteraization of land surface evaporation by means of location dependent potential evaporation and surface temperature range. In *Exchange Processes at the Land Surface for a Range of Space and Time Scales*; IAHS Press: Wallingford, UK, 1993.
45. Bastiaanssen, W.G.M.; Menenti, M.; Feddes, R.A.; Holtslag, A.A.M. A remote sensing surface energy balance algorithm for land (SEBAL). 1. Formulation. *J. Hydrol.* **1998**, *212*, 198–212. [CrossRef]
46. Bastiaanssen, W.G.M.; Pelgrum, H.; Wang, J.; Ma, Y.; Moreno, J.F.; Roerink, G.J.; Van der Wal, T. A remote sensing surface energy balance algorithm for land (SEBAL). 2. Validation. *J. Hydrol.* **1998**, *212*, 213–229. [CrossRef]
47. Roerink, G.J.; Su, Z.; Menenti, M. S-SEBI: A simple remote sensing algorithm to estimate the surface energy balance. *Phys. Chem. Earth Part B Hydrol. Ocean. Atmos.* **2000**, *25*, 147–157. [CrossRef]
48. Su, Z. The Surface Energy Balance System (SEBS) for estimation of turbulent heat fluxes. *Hydrol. Earth Syst. Sci.* **2002**, *6*, 85–100. [CrossRef]
49. Allen, R.G.; Tasumi, M.; Trezza, R. Satellite-based energy balance for mapping evapotranspiration with internalized calibration (METRIC)—Model. *J. Irrig. Drain. Eng.* **2007**, *133*, 380–394. [CrossRef]
50. Pelgrum, H.; Miltenburg, I.; Cheema, M.; Klaasse, A.; Bastiaanssen, W. ETLook a novel continental evapotranspiration algorithm. In Proceedings of the Remote Sensing and Hydrology Symposium, Jackson Hole, WY, USA, 27–30 September 2010; Volume 10875, p. 1087.
51. Senay, G.B.; Bohms, S.; Singh, R.K.; Gowda, P.H.; Velpuri, N.M.; Alemu, H.; Verdin, J.P. Operational Evapotranspiration Mapping Using Remote Sensing and Weather Datasets: A New Parameterization for the SSEB Approach. *Jawra J. Am. Water Resour. Assoc.* **2013**, *49*, 577–591. [CrossRef]
52. Yilmaz, M.T.; Anderson, M.C.; Zaitchik, B.; Hain, C.R.; Crow, W.T.; Ozdogan, M.; Chun, J.A.; Evans, J. Comparison of prognostic and diagnostic surface flux modeling approaches over the Nile River basin. *Water Resour. Res.* **2014**, *50*, 386–408. [CrossRef]
53. Mu, Q.; Heinsch, F.A.; Zhao, M.; Running, S.W. Development of a global evapotranspiration algorithm based on MODIS and global meteorology data. *Remote Sens. Environ.* **2007**, *111*, 519–536. [CrossRef]
54. Mu, Q.; Zhao, M.; Running, S.W. Improvements to a MODIS global terrestrial evapotranspiration algorithm. *Remote Sens. Environ.* **2011**, *115*, 1781–1800. [CrossRef]
55. FAO. *Using Remote Sensing in Support of Solutions to Reduce Agricultural Water Productivity Gaps. DATABASE Methodology*; FAO: Rome, Italy, 2018.
56. Miralles, D.G.; Holmes, T.R.H.; Jeu, R.A.M.D.; Gash, J.H.; Meesters, A.G.C.A.; Dolman, A.J. Global land-surface evaporation estimated from satellite-based observations. *Hydrol. Earth Syst. Sci.* **2011**, *15*, 453–469. [CrossRef]

57. Martens, B.; Miralles, D.; Lievens, H.; Fernández-Prieto, D.; Verhoest, N.E.C. Improving terrestrial evaporation estimates over continental Australia through assimilation of SMOS soil moisture. *Int. J. Appl. Earth Obs. Geoinf.* **2016**, *48*, 146–162. [CrossRef]
58. Martens, B.; Miralles, D.G.; Lievens, H.; van der Schalie, R.; de Jeu, R.A.M.; Fernández-Prieto, D.; Beck, H.E.; Dorigo, W.A.; Verhoest, N.E.C. GLEAM v3: Satellite-based land evaporation and root-zone soil moisture. *Geosci. Model Dev.* **2017**, *10*, 1903–1925. [CrossRef]
59. EUMETSAT. *SAF for Land Surface Analysis (LSA SAF). Algorithm Theoretical Basis Document Meteosat Second Generation Based Products*; EUMETSAT: Lisbon, Portugal, 2016.
60. Norman, J.M.; Kustas, W.P.; Humes, K.S. Source approach for estimating soil and vegetation energy fluxes in observations of directional radiometric surface temperature. *Agric. For. Meteorol.* **1995**, *77*, 263–293. [CrossRef]
61. Droogers, P.; Immerzeel, W.; Perry, C. Application of remote sensing in national water plans: Demonstration cases for Egypt, Saudi-Arabia and Tunisia. *Rep. FutureWater* **2009**, *80*. Available online: https://www.futurewater.eu/projects/remote-sensing-nwp-2/ (accessed on 5 September 2019).
62. Farg, E.; Arafat, S.M.; Abd El-Wahed, M.S.; EL-Gindy, A.M. Estimation of Evapotranspiration ETc and Crop Coefficient Kc of Wheat, in south Nile Delta of Egypt Using integrated FAO-56 approach and remote sensing data. *Egypt. J. Remote Sens. Space Sci.* **2012**, *15*, 83–89. [CrossRef]
63. Bastiaanssen, W.G.M.; Karimi, P.; Rebelo, L.-M.; Duan, Z.; Senay, G.; Muthuwatte, L.; Smakhtin, V. Earth Observation Based Assessment of the Water Production and Water Consumption of Nile Basin Agro-Ecosystems. *Remote Sens.* **2014**, *6*, 10306–10334. [CrossRef]
64. Elnmer, A.; Khadr, M.; Kanae, S.; Tawfik, A. Mapping daily and seasonally evapotranspiration using remote sensing techniques over the Nile delta. *Agric. Water Manag.* **2019**, *213*, 682–692. [CrossRef]
65. Yates, D.N.; Strzepek, K.M. An Assessment of Integrated Climate Change Impacts on the Agricultural Economy of Egypt. *Clim. Chang.* **1998**, *38*, 261–287. [CrossRef]
66. Hereher, M.E. The status of Egypt's agricultural lands using MODIS Aqua data. *Egypt. J. Remote Sens. Space Sci.* **2013**, *16*, 83–89. [CrossRef]
67. Maqbool, M.A.; Kerry, B. *Plant Nematode Problems and Their Control in the Near East Region: Proceedings*; FAO: Rome, Italy, 1997.
68. Friedl, M.A.; Sulla-Menashe, D.; Tan, B.; Schneider, A.; Ramankutty, N.; Sibley, A.; Huang, X. MODIS Collection 5 global land cover: Algorithm refinements and characterization of new datasets. *Remote Sens. Environ.* **2010**, *114*, 168–182. [CrossRef]
69. Friedl, M.; Sulla-Menashe, D. MCD12Q1 MODIS/Terra+Aqua Land Cover Type Yearly L3 Global 500m SIN Grid V006 (Data Set). NASA EOSDIS Land Processes DAAC. 2015. Available online: https://lpdaac.usgs.gov/products/mcd12q1v006/ (accessed on 25 September 2018).
70. Al Zayed, I.S.; Elagib, N.A.; Ribbe, L.; Heinrich, J. Spatio-temporal performance of large-scale Gezira Irrigation Scheme, Sudan. *Agric. Syst.* **2015**, *133*, 131–142. [CrossRef]
71. Khalifa, M.; Elagib, N.A.; Ribbe, L.; Schneider, K. Spatio-temporal variations in climate, primary productivity and efficiency of water and carbon use of the land cover types in Sudan and Ethiopia. *Sci. Total Environ.* **2018**, *624*, 790–806. [CrossRef]
72. METRIC-EEFLUX. Available online: https://eeflux-level1.appspot.com/ (accessed on 20 September 2018).
73. Allen, R.G.; Morton, C.; Kamble, B.; Kilic, A.; Huntington, J.; Thau, D.; Gorelick, N.; Erickson, T.; Moore, R.; Trezza, R. EEFlux: A Landsat-based evapotranspiration mapping tool on the Google Earth Engine. In Proceedings of the 2015 ASABE/IA Irrigation Symposium: Emerging Technologies for Sustainable Irrigation-A Tribute to the Career of Terry Howell, Sr. Conference Proceedings, Long Beach, CA, USA, 10–12 November 2015; pp. 1–11.
74. FEWS Home. Early Warning and Environmental Monitoring Program. Available online: https://earlywarning.usgs.gov/fews (accessed on 21 September 2018).
75. Numerical Terradynamic Simulation Group. MODIS Global Evapotranspiration Project (MOD16). Available online: https://www.ntsg.umt.edu/project/modis/mod16.php (accessed on 23 September 2018).
76. Monteith, J.L. *Evaporation and Environment. The State and Movement of Water in Living Organisms. Symposium of the Society of Experimental Biology*; Cambridge University Press: Cambridge, UK, 1965; Volume 19, pp. 205–234.

77. Didan, K. MOD13A3 MODIS/Terra Vegetation Indices Monthly L3 Global 1km SIN Grid V006 (Data Set). NASA EOSDIS Land Processes DAAC. 2015. Available online: https://lpdaac.usgs.gov/products/mod13a3v006/ (accessed on 25 September 2018).
78. European Space Agency Data User Element. ESA Data User Element. Available online: http://due.esrin.esa.int/page_globcover.php (accessed on 27 September 2018).
79. Central Agency for Public Mobilization and Statistics (CAPMAS). Cultivated Area. Available online: http://www.capmas.gov.eg/Pages/IndicatorsPage.aspx?page_id=6151&ind_id=2361 (accessed on 25 September 2018).
80. Central Agency for Public Mobilization and Statistics (CAPMAS). Home Page. Available online: http://www.capmas.gov.eg/HomePage.aspx (accessed on 25 September 2018).
81. ArcGIS. Mapping & Analytics Platform. Available online: https://www.esri.com/en-us/arcgis/about-arcgis/overview (accessed on 30 November 2018).
82. USGS SLC-off Products. Available online: https://www.usgs.gov/faqs/what-landsat-7-etm-slc-data?qt-news_science_products=0#qt-news_science_products (accessed on 30 October 2018).
83. USGS Which Images Will Work Best to Fill in the Gaps in Landsat 7 ETM+ SLC-off Images. Available online: https://landsat.usgs.gov/which-images-will-work-best-fill-gaps (accessed on 30 October 2018).
84. Sun, R.; Gao, X.; Liu, C.-M.; Li, X.-W. Evapotranspiration estimation in the Yellow River Basin, China using integrated NDVI data. *Int. J. Remote Sens.* **2004**, *25*, 2523–2534. [CrossRef]
85. Pringle, M.J. Robust prediction of time-integrated NDVI. *Int. J. Remote Sens.* **2013**, *34*, 4791–4811. [CrossRef]
86. Central Agency for Public Mobilization and Statistics (CAPMAS). Annual Bulletin of Irrigation and Water Resources Statistics. Available online: http://www.capmas.gov.eg/Pages/Publications.aspx?page_id=5104&YearID=23324 (accessed on 5 October 2018).
87. Sakthivadivel, R.; Merrey, D.J.; Fernando, N. Cumulative relative water supply: A methodology for assessing irrigation system performance. *Irrig. Drain. Syst.* **1993**, *7*, 43–67. [CrossRef]
88. Malano, H.; Burton, M. *Guidelines for Benchmarking Performance in the Irrigation and Drainage Sector*; FAO: Rome, Italy, 2001.
89. Bandara, K.M.P.S. Monitoring irrigation performance in Sri Lanka with high-frequency satellite measurements during the dry season. *Agric. Water Manag.* **2003**, *58*, 159–170. [CrossRef]
90. Salvador, R.; Martínez-Cob, A.; Cavero, J.; Playán, E. Seasonal on-farm irrigation performance in the Ebro basin (Spain): Crops and irrigation systems. *Agric. Water Manag.* **2011**, *98*, 577–587. [CrossRef]
91. Moreno-Pérez, M.F.; Roldán-Cañas, J. Assessment of irrigation water management in the Genil-Cabra (Córdoba, Spain) irrigation district using irrigation indicators. *Agric. Water Manag.* **2013**, *120*, 98–106. [CrossRef]
92. Simonneaux, V.; Abdrabbo, M.A.A.; Saleh, S.M.; Hassanein, M.K.; Abou-Hadid, A.F.; Chehbouni, A. MODIS estimates of annual evapotranspiration of irrigated crops in the Nile delta based on the FAO method: Application to the Nile river budget. *Proc. SPIE* **2010**, *7824*, 78241S.
93. Bekele, S.; Smakhtin, V.U.; Molden, D.J.; Peden, D.G. *The Nile River Basin: Water, Agriculture, Governance and Livelihoods*; Routledge: Abingdon, UK, 2012.
94. Elhag, M.; (King Abdulaziz University, Jeddah, Saudi Arabia). Personal communication, 2018.
95. Wheeler, K.G.; Basheer, M.; Mekonnen, Z.T.; Eltoum, S.O.; Mersha, A.; Abdo, G.M.; Zagona, E.A.; Hall, J.W.; Dadson, S.J. Cooperative filling approaches for the Grand Ethiopian Renaissance Dam. *Water Int.* **2016**, *41*, 611–634. [CrossRef]
96. Mahmoud, M.A.; El-Bably, A.Z. Crop Water Requirements and Irrigation Efficiencies in Egypt. In *Conventional Water Resources and Agriculture in Egypt*; The Handbook of Environmental Chemistry; Negm, A.M., Ed.; Springer International Publishing: Cham, Switzerland, 2019; pp. 471–487, ISBN 978-3-319-95065-5.
97. El-Din, M.N. Proposed climate change adaptation strategy for the ministry of water resources & irrigation in Egypt. *Joint Programme for Climate Change Risk Management in EGYPT*. 2013. Available online: http://www.eeaa.gov.eg/portals/0/eeaaReports/CCRMP/7.%20CC%20Water%20Strategy/CC%20Final%20Submitted%208-March%202013%20AdptStrtgy.pdf (accessed on 8 June 2019).

98. Ha, V.T.T. Water saving through reuse of return flow in paddy fields. In *Making Sense of Research for Sustainable Land Management*; Liniger, H., Mekdaschi, R., Moll, P., Zander, U., Eds.; Centre for Development and Environment (CDE), University of Bern, Switzerland and Helmholtz-Centre for Environmental Research GmbH–UFZ: Leipzig, Germany, 2017; Part 2, pp. 271–274.
99. Ha, V.T.T.; Quoc, V.T.; Ribbe, L. Reuse potential of return flow for irrigating paddy farms in the Vu Gia Thu Bon Delta, Central Vietnam. *J. Int. Sci. Publ.* **2017**, *5*, 346–360.